J. Plasma Phys. (2022), *vol*. 88, 905880101
Published by Cambridge University Press.

doi:10.1017/S0022377821001227

Propagation characteristics of parallel propagating waves in a relativistic magnetized electron plasma

Waseem Khan [1], M Ali [2], Ayesha Kanwal[2], Huzaifa Bilal[2], Tajammal H. Khokhar [2] and Yousaf Habib[3]

[1]Department of Physical Electronics, Faculty of Science, Masaryk University, Kotlářská 2, Brno 611 37, Czech Republic

[2]School of Natural Sciences (SNS), National University of Sciences and Technology (NUST), Islamabad 44000, Pakistan

[3]Department of Mathematics, COMSATS University Islamabad, Lahore Campus, Lahore, Pakistan

(Received 6 July 2021; revised 3 November 2021; accepted 10 November 2021)

Propagation characteristics (propagation regions and cutoffs) of parallel propagating modes (Langmuir, right- and left-handed circularly polarized waves) are studied for relativistic, weakly relativistic and non-relativistic magnetized electron plasma using the kinetic model. The dispersion relation for parallel propagating modes in relativistic electron plasma is investigated by employing the Maxwell–Boltzmann–J üttner distribution function and the final dispersion relation obtained is more general since no approximation is used. As the integrals in the relativistic dispersion relation cannot be done analytically so these integrals have been solved with the numerical quadrature approach. For $\eta \leq 1$ (ratio of rest mass energy to thermal energy), the increase in the effective mass of electrons will result in a change in the mass-dependent quantities (plasma frequency, electron cyclotron frequency, electron sound velocity, etc.) which in turn significantly affect the propagation characteristics of parallel propagating modes. It is observed that the propagation region for these parallel propagating modes decreases and cutoff points are shifted to lower values when we consider a relativistic plasma environment. Moreover, a low-density and high-temperature plasma is more transparent as compared with a high-density and low-temperature plasma for these modes.

1. Introduction

Plasma parameters like density, magnetic field and temperature vary over a wide range in various space and laboratory plasma environments. On the basis of these parameters we can classify these environments as being non-relativistic, weakly relativistic, relativistic, degenerate, relativistic degenerate, magnetized, cold and hot plasmas. The characteristics of the waves (propagation, cutoff and resonance) are modified in these plasma environments since the plasma frequency, thermal velocity and cyclotron frequency do not remain the same. In a plasma environment, the relativistic effects become prominent when thermal energy (k_BT) of the particles approaches their rest mass energy (m_oc^2) (Hazeltine & Waelbroeck 2018) and in turn the linear and nonlinear behaviour of plasma

waves is strongly influenced (Pelletier & Marcowith 1998; Ghosh *et al.* 2012). Magnetized relativistic environments are known to exist in different situations like in active galactic nuclei (jets produced by the rotation of heavy black holes) (Petropoulou *et al.* 2019), other astrophysical objects (such as neutron stars, pulsars, micro-quasars, etc.) (Beskin *et al.* 1988; Chabrier *et al.* 2002; Melrose 2017) and Van Allen radiation belts (Horne *et al.* 2005), and also have primary importance in tokamak plasmas (Bandaru *et al.* 2019) and laser–plasma interactions (Banerjee *et al.* 2002).

Extensive literature is available which discusses parallel propagating waves in relativistic plasma environments under certain conditions and limitations. Lerche (1968) discussed these waves in a relativistic environment and found that there will be resonant diffusion only when relativistic particles are present. He used the assumptions of ultra-relativistic plasma and high-phase refractive index. Melrose & Gedalin (1999) used the relativistic plasma dispersion function to derive the properties of these waves in the extremely relativistic case. Asenjo *et al.* (2009) used magnetofluid unification formalism to derive the dispersion relation of circularly polarized waves along a constant magnetic field. It was concluded that when relativistic effects are larger the electromagnetic wave becomes a non-dispersive light wave. The particle velocities are assumed to be purely transverse with respect to the magnetic field which means that no pressure or density fluctuation is considered. Lazar & Schlickeiser (2006) derived a relativistically correct dispersion relation of parallel propagating waves in magnetized thermal plasma of non-relativistic temperature. Schlickeiser (1998) solved the dispersion relation of parallel propagating waves analytically for the case of superluminal (waves with phase speed greater than the speed of light) and subluminal (waves with phase speed less than the speed of light) waves. Abbas *et al.* (2012) discussed both parallel and perpendicular propagating waves in weakly magnetized relativistic plasma under various limits and observed that the propagation region broadens as the plasma environment gets more relativistic. Khan *et al.* (2020*a*) applied the weak magnetic field limit on parallel propagating waves in a relativistic plasma environment and found a shift in cutoff points towards lower values of the frequency. Sazhin (1987) presented an approximate analysis of different types of electromagnetic wave propagation in a weakly relativistic electron plasma. He deduced that in the vicinity of certain frequencies, relativistic effects on the refractive index of these waves cannot be disregarded even when the electron energy is quite small. He concluded that the frequencies corresponding to the cutoffs in a weakly relativistic plasma are shifted compared with the frequencies corresponding to the cutoffs in a cold plasma, so that the frequency range of possible wave propagation increases.

We do find research articles where the dispersion relation of parallel propagating modes in a relativistic plasma environment is derived but, unfortunately, in order to solve the integral that contains relativistic momentum (which cannot be solved analytically) certain approximations ($\omega < kv,\ \omega > kv$) are used. However, we have tried to solve these integrals numerically without using any approximation. There has been extensive work done by Kepppens *et al.* to present a relativistically complete two-fluid analysis for a pair plasma. They discuss the advantages of using the governing 12th-degree polynomial in the wave frequency ω which represents 12 non-trivial waves and that can be separated into six pairs of forward- and backward-propagating waves, as the polynomial is sixth order in ω^2 (Keppens & Goedbloed 2019; Keppens *et al.* 2019; De Jonghe & Keppens 2020). But we know that an ideal two-fluid viewpoint fails to describe wave–particle interactions. So, we cannot discuss wave propagation for different particle velocities using this model.

The paper is organized as follows. Section 2 consists of the general formalism and dispersion relation for parallel propagating waves. The numerical approach we use is

https://doi.org/10.1017/S0022377821001227 Published online by Cambridge University Press

presented in § 3 and § 4 deals with the graphical analysis and discussion. Lastly, § 5 presents the conclusion of our paper.

2. Parallel propagating waves in magnetized relativistic plasma

The generalized expression for the plasma conductivity tensor (Abbas *et al.* 2012; Khan *et al.* 2020*a*) is given as

$$\sigma_{\alpha\beta} = \sum_s \frac{q^2 n_0}{\omega} \int_0^\infty \int_0^\pi \int_0^{2\pi} p^2 \sin\theta \, \mathrm{d}\theta \, \mathrm{d}p \, \mathrm{d}\phi' \frac{v_\alpha}{\Omega}$$
$$\int_{-\infty}^{\phi} \mathrm{d}\phi' \exp\left[\frac{1}{\Omega}((-\mathrm{i}\omega + \mathrm{i}k_z v\cos\theta)(\phi - \phi')\right.$$
$$\left. + \mathrm{i}k_x v \sin\theta(\sin\phi - \sin\phi'))\right]\left[(\omega - \boldsymbol{k}\cdot\boldsymbol{v})\frac{\partial f_o}{\partial p_\beta} + v_\beta\left(\boldsymbol{k}\cdot\frac{\partial f_o}{\partial \boldsymbol{p}}\right)\right]. \tag{2.1}$$

Here q, n_0, Ω, $\sum_s$ and f_0 are the electron charge, equilibrium number density, relativistic cyclotron frequency, sum over species and equilibrium distribution function, respectively. The velocity $\boldsymbol{v}$ in spherical coordinates is given as

$$\boldsymbol{v} = (v\sin\theta\cos\phi, v\sin\theta\sin\phi, v\cos\theta). \tag{2.2}$$

The wave vector $\boldsymbol{k}$ for parallel propagation is taken as

$$\boldsymbol{k} = k_z\hat{z}. \tag{2.3}$$

The relativistic velocity $\boldsymbol{v}$ and the relativistic cyclotron frequency Ω are defined as

$$v = \frac{cp}{(m^2c^2 + p^2)}^{1/2} \tag{2.4}$$

and

$$\Omega = \frac{\omega_{ce}}{\gamma}, \tag{2.5}$$

where γ is the relativistic factor given as

$$\gamma = \left(1 + \frac{p^2}{m^2c^2}\right)^{1/2}. \tag{2.6}$$

Here we are considering electron–ion plasma but since the waves under our consideration are high-frequency waves so ion dynamics is not included. This is the reason why we drop the summation over the species from now on. To derive the dispersion relation for parallel propagating waves the following dyadic is used (Montgomery & Tidman 1964; Schlickeiser 1998):

$$R_{\alpha\beta} = (\omega^2 - c^2k^2)\delta_{\alpha\beta} + c^2k_\alpha k_\beta + 4\pi\iota\omega\sigma_{\alpha\beta}; \tag{2.7}$$

and we take propagation vector $\boldsymbol{k}$ in the direction of magnetic field $\boldsymbol{B}$ that is in the z direction. So the required components of the dyadic are given as

$$R_{xx} = \omega^2 - c^2k^2 + 4\pi\iota\omega\sigma_{xx}, \tag{2.8}$$

https://doi.org/10.1017/S0022377821001227 Published online by Cambridge University Press

$$R_{xy} = -R_{yx} = 4\pi\iota\omega\sigma_{xy}, \tag{2.9}$$

$$R_{zz} = \omega^2 + 4\pi\iota\omega\sigma_{zz}, \tag{2.10}$$

where σ_{xx}, σ_{xy} and σ_{zz} are components of the conductivity tensor and are written as

$$\sigma_{xx} = -q^2 n_0 \int_0^\infty p^2 \frac{\partial f_0}{\partial p}\,\mathrm{d}p \int_0^\pi \frac{v}{\Omega}\sin^3\theta\,\mathrm{d}\theta \int_0^{2\pi} \cos\phi \times \cos(\phi-\alpha)\,\mathrm{d}\phi \int_\infty^0 \exp\left[\frac{-\mathrm{i}}{\Omega}(\omega - k_z v\cos\theta)\alpha\right]\mathrm{d}\alpha, \tag{2.11}$$

$$\sigma_{xy} = -q^2 n_0 \int_0^\infty p^2 \frac{\partial f_0}{\partial p}\,\mathrm{d}p \int_0^\pi \frac{v}{\Omega}\sin^3\theta\,\mathrm{d}\theta \int_0^{2\pi} \cos\phi \times \sin(\phi-\alpha)\,\mathrm{d}\phi \int_\infty^0 \exp\left[\frac{-\mathrm{i}}{\Omega}(\omega - k_z v\cos\theta)\alpha\right]\mathrm{d}\alpha \tag{2.12}$$

and

$$\sigma_{zz} = -q^2 n_0 \int_0^\infty p^2 \frac{\partial f_0}{\partial p}\,\mathrm{d}p \int_0^\pi \frac{v}{\Omega}\cos^2\theta\sin\theta\,\mathrm{d}\theta \int_0^{2\pi} \mathrm{d}\phi \int_\infty^0 \exp\left[\frac{-\mathrm{i}}{\Omega}(\omega - k_z v\cos\theta)\alpha\right]\mathrm{d}\alpha. \tag{2.13}$$

By using the integrals

$$\int_0^{2\pi} \cos\phi\cos(\phi-\alpha)\,\mathrm{d}\phi = \pi\cos\alpha, \tag{2.14}$$

$$\int_\infty^0 \cos\alpha\exp\left[\frac{-\mathrm{i}}{\Omega}(\omega - k_z v\cos\theta)\alpha\right]\mathrm{d}\alpha = \frac{\mathrm{i}\Omega(\omega - k_z v\cos\theta)}{(\omega - k_z v\cos\theta)^2 - \Omega^2} \tag{2.15}$$

in (2.11) and after performing θ integration we can write

$$\sigma_{xx} = -n_0\,\mathrm{e}^2\,\mathrm{i}\pi \int_0^\infty p^2 \frac{\partial f_0}{\partial p}\,\mathrm{d}p \frac{1}{2k_z^3 v^2}\Bigg(4k_z v\omega + (\omega - k_z v - \Omega)(\omega - k_z v - \Omega)\log\left[\frac{\omega - k_z v - \Omega}{\omega + k_z v - \Omega}\right] + (\omega - k_z v + \Omega)(\omega + k_z v + \Omega)\log\left[\frac{\omega - k_z v + \Omega}{\omega + k_z v + \Omega}\right]\Bigg). \tag{2.16}$$

Similarly, the other two components can also be simplified as

$$\sigma_{xy} = -n_0\,\mathrm{e}^2\pi \int_0^\infty p^2 \frac{\partial f_0}{\partial p}\,\mathrm{d}p \frac{1}{2k_z^3 v^2}\Bigg(4k_z v\Omega - (\omega - k_z v - \Omega)(\omega + k_z v - \Omega)\log\left[\frac{\omega - k_z v - \Omega}{\omega + k_z v - \Omega}\right] + (\omega - k_z v + \Omega)(\omega + k_z v + \Omega)\log\left[\frac{\omega - k_z v + \Omega}{\omega + k_z v + \Omega}\right]\Bigg) \tag{2.17}$$

https://doi.org/10.1017/S0022377821001227 Published online by Cambridge University Press

and

$$\sigma_{zz} = -2n_0\,\mathrm{e}^2\,\mathrm{i}\pi\int_0^\infty p^2\frac{\partial f_0}{\partial \boldsymbol{p}}\,\mathrm{d}p\left(\frac{\omega^2}{k_z^3v^3}\left(2\frac{k_zv}{\omega}+\log\left[\frac{\omega-k_zv}{\omega+k_zv}\right]\right)\right). \tag{2.18}$$

Classical non-interacting particles at thermal equilibrium can be described by the Maxwell–Boltzmann distribution whereas to include the relativistic effects we need to use the Maxwell–Jüttner equilibrium distribution function (MJDF) (Buti 1963; Montgomery & Tidman 1964; Georgiou 1996; Ali *et al.* 2019; Khan *et al.* 2020*b*,*c*), given as

$$f_0(\boldsymbol{p}) = \frac{1}{4\pi m^3c^3}\frac{\eta}{K_2(\eta)}\exp[-\eta\gamma], \tag{2.19}$$

where $\eta = mc^2/k_BT$ (ratio of rest mass energy to thermal energy) and K_2 is the modified Bessel function of the second kind of order two.

After substituting the MJDF in (2.16)–(2.18) and using the obtained values of σ_{xx}, σ_{xy} and σ_{zz} in (2.8), (2.9) and (2.10), respectively, we get

$$\begin{aligned}
R_{xx} = {}& \omega^2 - c^2k_z^2 - \frac{\omega_{pe}^2}{8}\frac{\omega}{ck_z}\frac{\eta^2}{K_2(\eta)}\int_0^\infty z(1+z^2)^{1/2}\\
&\times\exp[-\eta(1+z^2)^{1/2}]\left(4\frac{\omega}{ck_z}\frac{z}{(1+z^2)^{1/2}}+\left(\frac{\omega}{ck_z}-\frac{z}{(1+z^2)^{1/2}}\right.\right.\\
&\left.-\frac{\omega_{ce}}{ck_z}\frac{1}{(1+z^2)^{1/2}}\right)\left(\frac{\omega}{ck_z}+\frac{z}{(1+z^2)^{1/2}}-\frac{\omega_{ce}}{ck_z}\frac{1}{(1+z^2)^{1/2}}\right)\\
&\log\left|\frac{\dfrac{\omega}{ck_z}-\dfrac{z}{(1+z^2)^{1/2}}-\dfrac{\omega_{ce}}{ck_z}\dfrac{1}{(1+z^2)^{1/2}}}{\dfrac{\omega}{ck_z}+\dfrac{z}{(1+z^2)^{1/2}}-\dfrac{\omega_{ce}}{ck_z}\dfrac{1}{(1+z^2)^{1/2}}}\right|+\left(\frac{\omega}{ck_z}-\frac{z}{(1+z^2)^{1/2}}\right.\\
&\left.\left.+\frac{\omega_{ce}}{ck_z}\frac{1}{(1+z^2)^{1/2}}\right)\left(\frac{\omega}{ck_z}+\frac{z}{(1+z^2)^{1/2}}+\frac{\omega_{ce}}{ck_z}\frac{1}{(1+z^2)^{1/2}}\right)\right.\\
&\left.\log\left|\frac{\dfrac{\omega}{ck_z}-\dfrac{z}{(1+z^2)^{1/2}}+\dfrac{\omega_{ce}}{ck_z}\dfrac{1}{(1+z^2)^{1/2}}}{\dfrac{\omega}{ck_zc+\dfrac{z}{(1+z^2)^{1/2}}+\dfrac{\omega_{ce}}{ck_z}\dfrac{1}{(1+z^2)^{1/2}}}}\right|\right)\mathrm{d}z,
\end{aligned} \tag{2.20}$$

$$\begin{aligned}
R_{xy} = -R_{yx} = {}& -\iota\frac{\omega_{pe}^2}{8}\frac{\omega}{ck_z}\frac{\eta^2}{K_2(\eta)}\int_0^\infty z(1+z^2)^{1/2}\\
&\times\exp[-\eta(1+z^2)^{1/2}]\left(4\frac{\omega_{ce}}{ck_z}\frac{z}{(1+z^2)}-\left(\frac{\omega}{ck_z}-\frac{z}{(1+z^2)^{1/2}}\right.\right.
\end{aligned}$$

https://doi.org/10.1017/S0022377821001227 Published online by Cambridge University Press

$$-\frac{\omega_{ce}}{ck_z}\frac{1}{(1+z^2)^{1/2}}\Bigg)\Bigg(\frac{\omega}{ck_z}+\frac{z}{(1+z^2)^{1/2}}-\frac{\omega_{ce}}{ck_z}\frac{1}{(1+z^2)^{1/2}}\Bigg)$$
$$\log\left|\frac{\frac{\omega}{ck_z}-\frac{z}{(1+z^2)^{1/2}}-\frac{\omega_{ce}}{ck_z}\frac{1}{(1+z^2)^{1/2}}}{\frac{\omega}{ck_z}+\frac{z}{(1+z^2)^{1/2}}-\frac{\omega_{ce}}{ck_z}\frac{1}{(1+z^2)^{1/2}}}\right|+\Bigg(\frac{\omega}{ck_z}-\frac{z}{(1+z^2)^{1/2}}$$
$$+\frac{\omega_{ce}}{ck_z}\frac{1}{(1+z^2)^{1/2}}\Bigg)\Bigg(\frac{\omega}{ck_z}+\frac{z}{(1+z^2)^{1/2}}+\frac{\omega_{ce}}{ck_z}\frac{1}{(1+z^2)^{1/2}}\Bigg)$$
$$\log\left|\frac{\frac{\omega}{ck_z}-\frac{z}{(1+z^2)^{1/2}}+\frac{\omega_{ce}}{ck_z}\frac{1}{(1+z^2)^{1/2}}}{\frac{\omega}{ck_z}+\frac{z}{(1+z^2)^{1/2}}+\frac{\omega_{ce}}{ck_z}\frac{1}{(1+z^2)^{1/2}}}\right|\Bigg)\,\mathrm{d}z \tag{2.21}$$

and

$$R_{zz}=\omega^2+\frac{\omega_{pe}^2}{2}\frac{\omega^3}{c^3k_z^3}\frac{\eta^2}{K_2(\eta)}\int_0^\infty z(1+z^2)^{1/2}\exp[-\eta(1+z^2)^{1/2}]$$
$$\times\left(2\frac{ck_z}{\omega}\frac{z}{(1+z^2)^{1/2}}+\log\left|\frac{\frac{\omega}{ck_z}-\frac{z}{(1+z^2)^{1/2}}}{\frac{\omega}{ck_z}+\frac{z}{(1+z^2)^{1/2}}}\right|\right)\mathrm{d}z, \tag{2.22}$$

where $z=p/mc$ and ω_{pe}, ω_{ce} are the plasma and cyclotron frequency of electrons, respectively. The integrals involved in (2.21), (2.22) and (3.1) cannot be done analytically, so these are computed numerically using the trapezoidal rule (Buti 1963; Evans 1993; Georgiou 1996; Burden & Faires 1997; Yang 2014; Ali *et al.* 2019; Khan *et al.* 2020*b*,*c*).

3. Dispersion relation

In this section we present the dispersion relation of the parallel propagating waves in magnetized fully relativistic plasma which can be analysed for relativistic ($\eta<1$), weakly relativistic ($\eta>1$) and non-relativistic ($\eta\gg1$) environments.

Langmuir waves. The dispersion relation for Langmuir waves is given as

$$R_{zz}=0. \tag{3.1}$$

Right- and left-hand circularly polarized modes. The dispersion relation for *R*-wave and *L*-wave is given as

$$R_{xx}\pm \mathrm{i}R_{xy}=0, \tag{3.2}$$

where the plus and minus signs represent right and left circularly polarized modes, respectively. The integrals involved in the dispersion relations cannot be solved analytically since no explicit anti-derivative exists for these integrals. However, we can solve these integrals numerically.

4. Discussion and graphical representation

As we know that the Langmuir mode remains unaffected by the magnetic field, so it is expected to get the same curves as presented in Khan *et al.* (2020*a*) for the case of the weak

https://doi.org/10.1017/S0022377821001227 Published online by Cambridge University Press

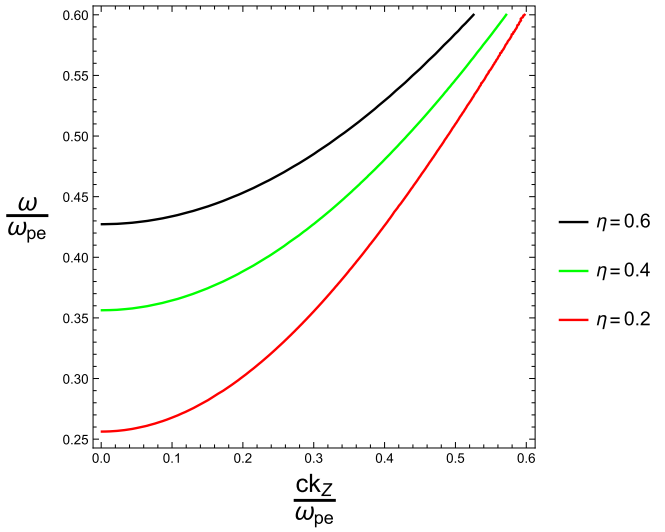

FIGURE 1. Dispersion curves showing solutions for Langumir waves in relativistic plasma for different values of η ($\eta = 0.2$, $\eta = 0.4$ and $\eta = 0.6$).

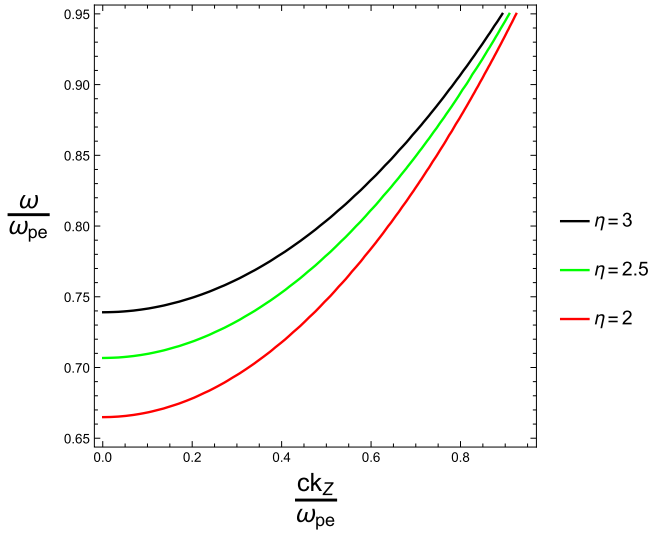

FIGURE 2. Dispersion curves showing solutions for Langumir waves in weakly relativistic plasma for different values of η ($\eta = 2$, $\eta = 2.5$ and $\eta = 3$).

magnetic field. However, the propagation of *R*- and *L*-waves depends on the magnetic field so the dispersion curves will be modified as we are not applying the weak field limit.

In figures 1–3, the dispersion curves for Langmuir waves are analysed for different environments, i.e. relativistic, weakly relativistic and non-relativistic depending on the value of $\eta = m_0c^2/k_BT$. On comparing these three environments, it is found that as the plasma environment becomes more relativistic the cutoff points are shifted towards lower frequencies and the propagation region of the Langmuir wave broadens as reported earlier (Khan *et al.* 2020*a*). However, the results presented here are more general since no approximation is used in deriving the dispersion relation. In figure 4, we tried to retrieve

https://doi.org/10.1017/S0022377821001227 Published online by Cambridge University Press

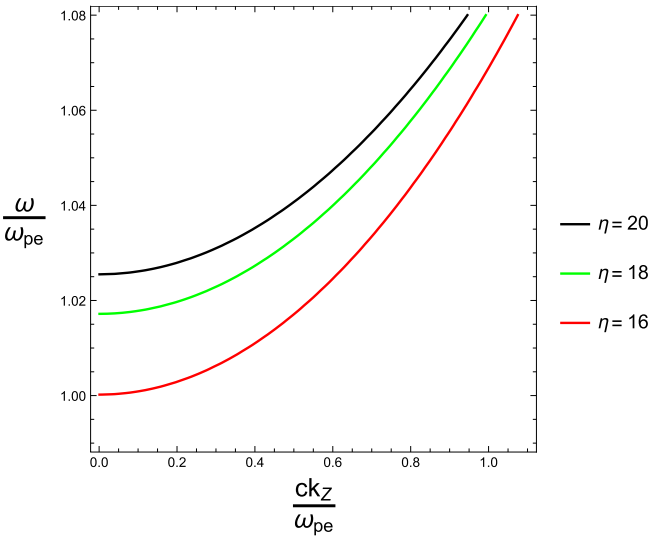

FIGURE 3. Dispersion curves showing solutions for Langumir waves in non-relativistic plasma for different values of η ($\eta = 16$, $\eta = 18$ and $\eta = 20$).

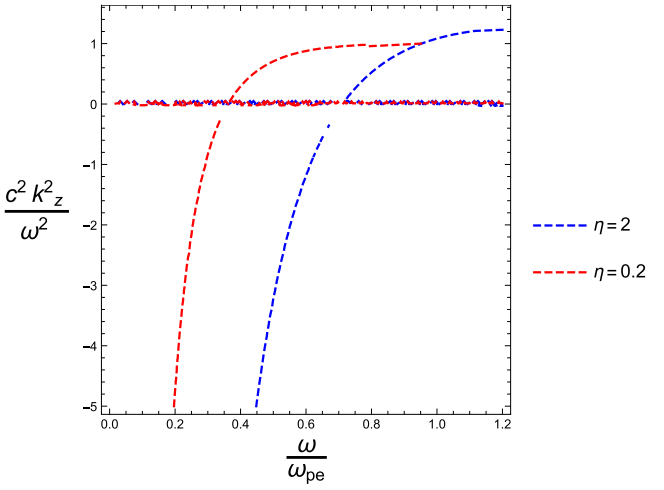

FIGURE 4. Dispersion curves showing solutions for Langumir waves in relativistic and weakly relativistic plasma for different values of η ($\eta = 0.2$ and $\eta = 2$).

the results of Melrose & Gedalin (1999). Here we plot the same graph as that given in the above mentioned reference but now we can discuss the variation in the dispersion curve for relativistic and weakly relativistic cases. As we decrease the value of η, i.e. we move towards the relativistic regime, the cutoff point (where the intersection of the relevant dotted line occurs) shifted to lower values of frequency or we can say that now the waves of lower values of frequency are allowed to propagate through the plasma.

In figures 5 and 6, the dispersion curves for *R*-wave are shown where we can observe that in both of these figures (with different ratio of density to magnetic field) the curves are shifted to the lower value of frequency as the plasma environment becomes more relativistic. This shifting of the curves is due to the fact that the cyclotron frequency of

https://doi.org/10.1017/S0022377821001227 Published online by Cambridge University Press

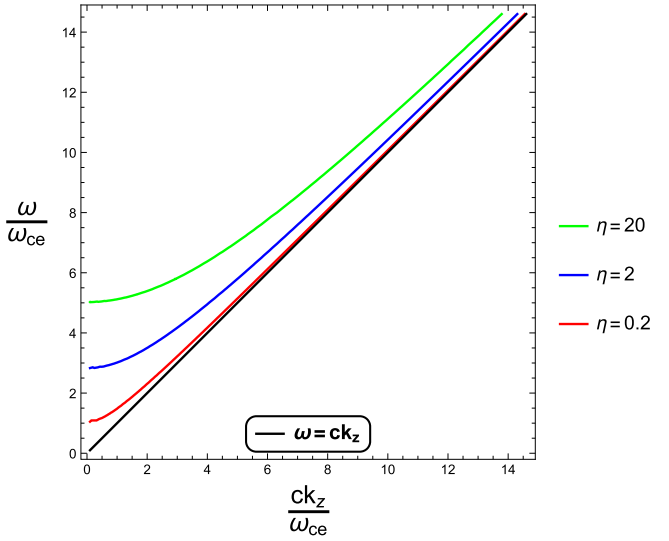

FIGURE 5. Dispersion curves showing solutions for *R*-mode in relativistic, weakly relativistic and non-relativistic plasma by taking ratio of $\omega_{pe}^2/\omega_{ce}^2 = 25$.

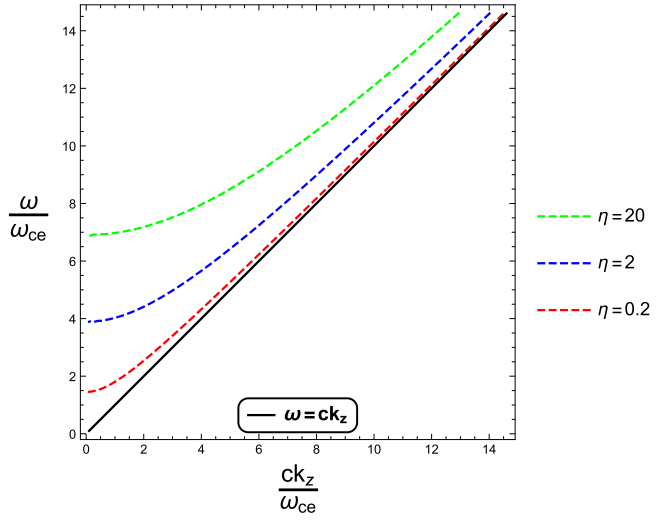

FIGURE 6. Dispersion curves showing solutions for *R*-mode in relativistic, weakly relativistic and non-relativistic plasma by taking ratio of $\omega_{pe}^2/\omega_{ce}^2 = 50$.

electrons reduces as the relativistic effects increase. We also observe that the plasma becomes transparent for the relativistic case much earlier, i.e. at lower values of k, as compared with the weakly relativistic or non-relativistic cases. Moreover, as the value of ω_p/ω_c increases, the density effects come in to play and the wave propagation shifts to higher values of frequency.

Similarly, the dispersion curves for the *L*-wave are shown in figures 7 and 8. The response of the *L*-wave to the relativistic effects and the ratio of density to magnetic field is the same as that of the *R*-wave. The plots presented in figures 9 and 10 show

https://doi.org/10.1017/S0022377821001227 Published online by Cambridge University Press

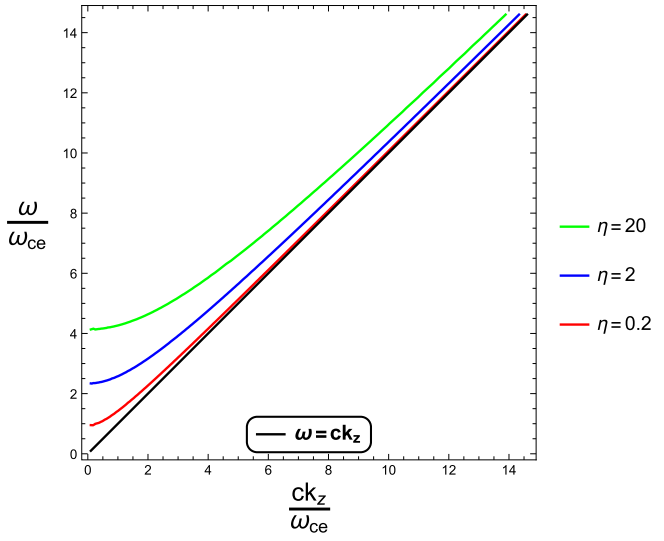

FIGURE 7. Dispersion curves showing solutions for L-mode in relativistic, weakly relativistic and non-relativistic plasma by taking ratio of $\omega_{pe}^2/\omega_{ce}^2 = 25$.

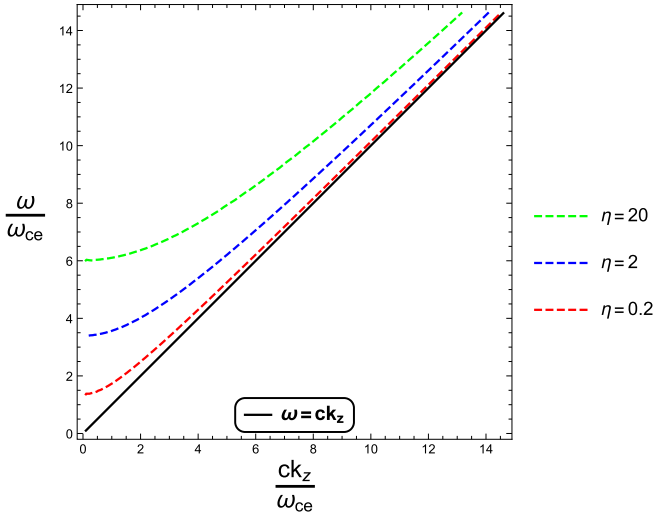

FIGURE 8. Dispersion curves showing solutions for L-mode in relativistic, weakly relativistic and non-relativistic plasma by taking ratio of $\omega_{pe}^2/\omega_{ce}^2 = 50$.

ω^2/c^2k^2 versus ω/ω_{ce} for a fixed value of $\omega_{pe}^2/\omega_{ce}^2$, a standard way of representing the propagation region for our wave of interest. Since the wave cannot propagate below the cutoff frequency,this represents a no-propagation region. The propagation region is the one where the wave frequency becomes larger than the cutoff frequency. Now with an increase in the relativistic factor η the cutoff point shifts to lower values of frequency, so the wave will start propagating at lower values of frequency which are not allowed in the non-relativistic case. This means that with the increase in the relativistic effects, the propagation region increases.

https://doi.org/10.1017/S0022377821001227 Published online by Cambridge University Press

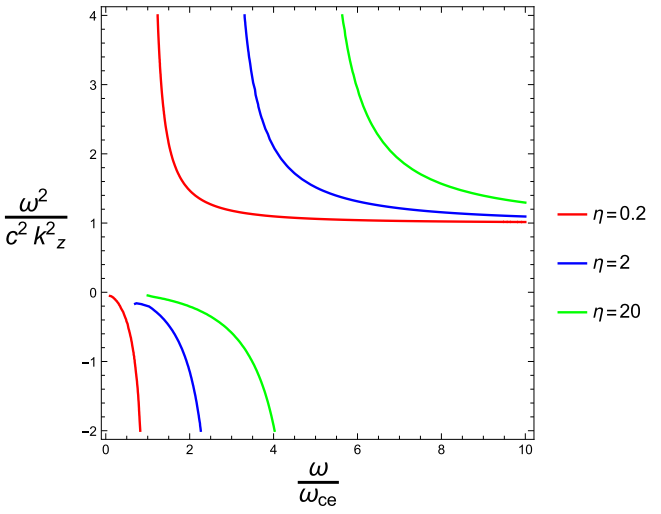

FIGURE 9. Dispersion curves showing the cutoffs of *R*-modes for relativistic plasma with $\omega_{pe}^2/\omega_{ce}^2 = 25$.

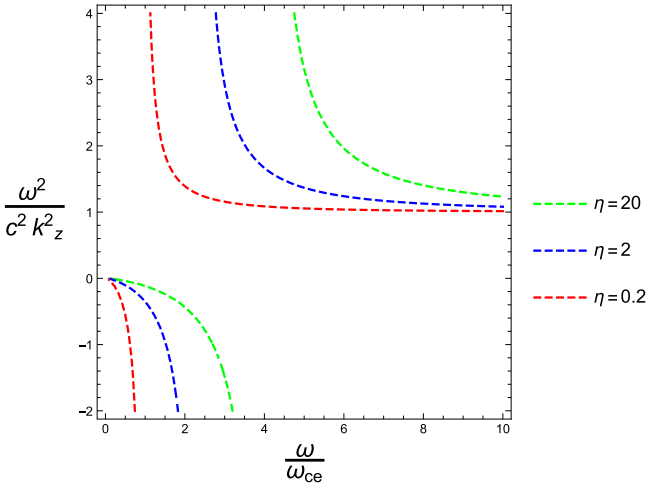

FIGURE 10. Dispersion curves showing the cutoffs of *L*-modes for relativistic plasma with $\omega_{pe}^2/\omega_{ce}^2 = 25$.

5. Conclusion

In this research work, we focus on relativistic plasmas which exist in many astrophysical (pulsars, quasars, active galactic nuclei, black holes, white dwarfs, neutron stars and radio galaxies) and laboratory (fusion experiment) environments. The increase in the effective mass not only depends on the the value of η but also depends on plasma density. Our analysis for parallel propagating waves in various relativistic plasma environments is very useful for scientists working in both space science and the laboratory setting. On the basis of our calculations, we conclude that the propagation region for parallel propagating waves is enhanced for relativistic and weakly relativistic plasma as compared with the non-relativistic plasma which means that now the wave can propagate at lower frequencies

https://doi.org/10.1017/S0022377821001227 Published online by Cambridge University Press

that were not allowed for propagation in the non-relativistic regime. We also observe that a low-density and high-temperature (relativistic) plasma environment is more transparent for the parallel propagating waves as compared with a high-density and low-temperature (weakly relativistic and non-relativistic) plasma environment.

Acknowledgements

Editor Antoine C. Bret thanks the referees for their advice in evaluating this article.

Declaration of interest

The authors report no conflict of interest.

Data availability

The data that support the findings of this study are available within the article.

REFERENCES

ABBAS, G., *et al.* 2012 Study of high frequency parallel propagating modes in a weakly magnetized relativistic degenerate electron plasma. *Phys. Plasmas* **19** (3), 032103.

ALI, M., *et al.* 2019 Propagation of Bernstein waves in weakly relativistic pair ion plasma. *Phys. Plasmas* **26** (10), 102101.

ASENJO, F., *et al.* 2009 Circularly polarized wave propagation in magnetofluid dynamics for relativistic electron-positron plasmas. *Phys. Plasmas* **16** (12), 122108.

BANDARU, V., *et al.* 2019 Simulating the nonlinear interaction of relativistic electrons and tokamak plasma instabilities: implementation and validation of a fluid model. *Phys. Rev.* E **99** (6), 063317.

BANERJEE, S., *et al.* 2002 High harmonic generation in relativistic laser–plasma interaction. *Phys. Plasmas* **9** (5), 2393–2398.

BESKIN, V.S., *et al.* 1988 Theory of the radio emission of pulsars. *AstroPhys. Space Sci*. **146** (2), 205–281.

BURDEN, R.L. & FAIRES, J.D. 1997 *Numerical Analysis*. Brooks/Cole.

BUTI, B. 1963 Relativistic effects on plasma oscillations and two-stream instability. I. *Phys. Fluids* **6** (1), 89–99.

CHABRIER, G., *et al.* 2002 Dense astrophysical plasmas. *J. Phys.: Condens. Matter* **14** (40), 9133.

DE JONGHE, J. & KEPPENS, R. 2020 A two-fluid analysis of waves in a warm ion–electron plasma. *Phys. Plasmas* **27** (12), 122107.

EVANS, G. 1993 *Practical Numerical Integration*. Wiley.

GEORGIOU, A. 1996 Dispersion relations for electron Bernstein waves in a relativistic plasma. *Plasma Phys. Control. Fusion* **38** (3), 347.

GHOSH, B., *et al.* 2012 Relativistic effects on the modulational instability of electron plasma waves in quantum plasma. *Pramana* **78** (5), 779–790.

HAZELTINE, R.D. & WAELBROECK, F.L. 2018 *The Framework of Plasma Physics*. CRC Press.

HORNE, R.B., *et al.* 2005 Wave acceleration of electrons in the Van Allen radiation belts. *Nature* **437** (7056), 227–230.

KEPPENS, R. & GOEDBLOED, H. 2019 A fresh look at waves in ion-electron plasmas. *Front. Astron. Space Sci*. **6**, 11.

KEPPENS, R., *et al.* 2019 Waves in a warm pair plasma: a relativistically complete two-fluid analysis. *J. Plasma Phys*. **85** (4).

KHAN, W., *et al.* 2020*a* Parallel propagating waves in weakly magnetized relativistic electron plasma. *IEEE Trans. Plasma Sci*. **48** (9), 2996–3000.

KHAN, W., *et al.* 2020*b* Electron cyclotron modes of Bernstein waves in different plasma environments. *Plasma Res. Express* **2** (1), 015004.

KHAN, W., *et al.* 2020*c* Characteristics of ordinary mode in fully relativistic electron plasma. *Plasma Phys. Control. Fusion* **62** (5), 055016.

LAZAR, M. & SCHLICKEISER, R. 2006 Relativistic kinetic dispersion theory of linear parallel waves in magnetized plasmas with isotropic thermal distributions. *New J. Phys*. **8** (5), 66.

LERCHE, I. 1968 Quasilinear theory of resonant diffusion in a magneto-active, relativistic plasma. *Phys. Fluid* **11** (8), 1720–1727.

MELROSE, D.B. 2017 Coherent emission mechanisms in astrophysical plasmas. *Rev. Mod. Plasma Phys*. **1** (1), 1–81.

MELROSE, D.B. & GEDALIN, M.E. 1999 Relativistic plasma emission and pulsar radio emission: a critique. *Astrophys. J*. **521** (1), 351.

MONTGOMERY, D.C. & TIDMAN, D.A. 1964 *Plasma Kinetic Theory*. McGraw-Hill.

PELLETIER, G. & MARCOWITH, A. 1998 Nonlinear dynamics in the relativistic plasma of astrophysical high-energy sources. *J. Astro phys*. **502** (2), 598.

PETROPOULOU, M., *et al.* 2019 Relativistic magnetic reconnection in electron–positron–proton plasmas: implications for jets of active galactic nuclei. *AstroPhys. J*. **880** (1), 37.

SAZHIN, S.S. 1987 An approximate theory of electromagnetic wave propagation in a weakly relativistic plasma. *J. Plasma Phys*. **37** (2), 209–230.

SCHLICKEISER, R. 1998 Relativistic kinetic theory of plasma waves. *Phys. Scr*. **1998** (T75), 33.

YANG, X.S. 2014 *Introduction to Computational Mathematics*. World Scientific Publishing Company.

https://doi.org/10.1017/S0022377821001227 Published online by Cambridge University Press